Inorganic Chemistry
Article

Inorg. Chem. **2010**, *49*, 10191–10198 **10191**
DOI: 10.1021/ic101501p

Coordination Networks from Cu Cations and Tetrakis(methylthio)benzenedicarboxylic Acid: Tunable Bonding Patterns and Selective Sensing for NH_3 Gas

Xiao-Ping Zhou,[†] Zhengtao Xu,[*,†] Jun He,[†] Matthias Zeller,[‡] Allen D. Hunter,[‡] Rodolphe Clérac,[§,∥] Corine Mathonière,[⊥] Stephen Sin-Yin Chui,[⊗] and Chi-Ming Che[⊗]

[†]*Department of Biology and Chemistry, City University of Hong Kong, 83 Tat Chee Avenue, Kowloon, Hong Kong, P.R. China,* [‡]*Department of Chemistry, Youngstown State University, One University Plaza, Youngstown, Ohio 44555, United States,* [§]*CNRS, UPR 8641, Centre de Recherche Paul Pascal (CRPP), Equipe "Matériaux Moléculaires Magnétiques", 115 avenue du Dr. Albert Schweitzer, 33600 Pessac, France,* [∥]*Université de Bordeaux, UPR 8641, Pessac F-33600, France,* [⊥]*CNRS UPR9048, Université Bordeaux, Institut de Chimie de la Matière Condensée de Bordeaux (ICMCB), 87 avenue du Dr. Albert Schweitzer, Pessac Cedex, F-33608, France, and* [⊗]*Department of Chemistry and HKU-CAS Joint Laboratory on New Materials, The University of Hong Kong, Pokfulam Road, Hong Kong, China*

Received July 27, 2010

This paper aims to illustrate the rich potential of the thioether-carboxyl combination in generating coordination networks with tunable and interesting structural features. By simply varying the ratio between $Cu(NO_3)_2$ and the bifunctional ligand tetrakis(methylthio)benzenedicarboxylic acid (TMBD) as the reactants, three coordination networks can be hydrothermally synthesized in substantial yields, which present a distinct evolution with regard to metal−ligand interactions. Specifically, $Cu(TMBD)_{0.5}(H_2TMBD)_{0.5}\cdot H_2TMBD$ (**1**) was obtained with a relatively small (1:1) $Cu(NO_3)_2$/TMBD ratio, and crystallizes as an one-dimensional (1D) coordination assembly based on Cu(I)-thioether interactions, which is integrated by hydrogen-bonding to additional H_2TMBD molecules to form a three-dimensional (3D) composite network with all the carboxylic acid and carboxylate groups remaining uncoordinated to the metal ions. A medium (1.25:1) $Cu(NO_3)_2$/TMBD ratio leads to compound Cu_2TMBD, in which Cu(I) ions simultaneously bond to the carboxylate and thioether groups, while an even higher (2.4:1) $Cu(NO_3)_2$/TMBD ratio produced a mixed-cation compound $Cu^{II}{}_2OHCu^{I}(TMBD)_2\cdot 2H_2O$ (**2**), in which the carboxylic groups are bonded to (cupric) Cu^{II} ions, and the thioether groups to Cu^{I}. Despite the lack of open channels in **2**, crystallites of this compound exhibit a distinct and selective absorption of NH_3, with a concomitant color change from green to blue, indicating substantial network flexibility and dynamics with regards to gas transport.

Introduction

Crystal engineering of extended networks[1] has entered a stage where it is ever more crucial to design and synthesize organic building blocks[2] with novel functional and structural features. We have extensively explored the advantages of aromatic thioethers for building complex, advanced

*To whom correspondence should be addressed. E-mail: zhengtao@cityu.edu.hk.

(1) (a) Batten, S. R.; Robson, R. *Angew. Chem., Int. Ed.* **1998**, *37*, 1461. (b) Carlucci, L.; Ciani, G.; Proserpio, D. M. *Coord. Chem. Rev.* **2003**, *246*, 247. (c) Kitagawa, S.; Kitaura, R.; Noro, S.-i. *Angew. Chem., Int. Ed.* **2004**, *43*, 2334. (d) Lee, S.; Mallik, A. B.; Xu, Z.; Lobkovsky, E. B.; Tran, L. *Acc. Chem. Res.* **2005**, *38*, 251. (e) Bradshaw, D.; Claridge, J. B.; Cussen, E. J.; Prior, T. J.; Rosseinsky, M. J. *Acc. Chem. Res.* **2005**, *38*, 273. (f) Suslick, K. S.; Bhyrappa, P.; Chou, J. H.; Kosal, M. E.; Nakagaki, S.; Smithenry, D. W.; Wilson, S. R. *Acc. Chem. Res.* **2005**, *38*, 283. (g) Mak, T. C. W.; Zhao, L. *Chem. Asian J.* **2007**, *2*, 456. (h) Ockwig, N. W.; Delgado-Friedrichs, O.; O'Keeffe, M.; Yaghi, O. M. *Acc. Chem. Res.* **2005**, *38*, 176. (i) Maspoch, D.; Ruiz-Molina, D.; Veciana, J. *Chem. Soc. Rev.* **2007**, *36*, 770. (j) Tanaka, D.; Kitagawa, S. *Chem. Mater.* **2008**, *20*, 922. (k) Férey, G. *Chem. Soc. Rev.* **2008**, *37*, 191. (l) Ma, L.; Abney, C.; Lin, W. *Chem. Soc. Rev.* **2009**, *38*, 1248. (m) Chen, B.; Xiang, S.; Qian, G. *Acc. Chem. Res.* **2010**, *43*, 1115.

(2) (a) Chen, Z.; Xiang, S.; Liao, T.; Yang, Y.; Chen, Y.-S.; Zhou, Y.; Zhao, D.; Chen, B. *Cryst. Growth Des.* **2010**, *10*, 2775. (b) Ma, L.; Mihalcik, D. J.; Lin, W. *J. Am. Chem. Soc.* **2009**, *131*, 4610. (c) Wu, C.-D.; Hu, A.; Zhang, L.; Lin, W. *J. Am. Chem. Soc.* **2005**, *127*, 8940. (d) Cui, Y.; Lee, S. J.; Lin, W. *J. Am. Chem. Soc.* **2003**, *125*, 6014. (e) Liu, Y.; Xu, X.; Zheng, F.; Cui, Y. *Angew. Chem., Int. Ed.* **2008**, *47*, 4538. (f) Ma, S.; Sun, D.; Ambrogio, M.; Fillinger, J. A.; Parkin, S.; Zhou, H.-C. *J. Am. Chem. Soc.* **2007**, *129*, 1858. (g) Sun, D.; Ma, S.; Ke, Y.; Collins, D. J.; Zhou, H.-C. *J. Am. Chem. Soc.* **2006**, *128*, 3896. (h) Nouar, F.; Eubank, J. F.; Bousquet, T.; Wojtas, L.; Zaworotko, M. J.; Eddaoudi, M. *J. Am. Chem. Soc.* **2008**, *130*, 1833. (i) Lin, X.; Blake, A. J.; Wilson, C.; Sun, X. Z.; Champness, N. R.; George, M. W.; Hubberstey, P.; Mokaya, R.; Schröder, M. *J. Am. Chem. Soc.* **2006**, *128*, 10745. (j) Koh, K.; Wong-Foy, A., G.; Matzger, A. J. *J. Am. Chem. Soc.* **2009**, *131*, 4184. (k) Zharkouskaya, A.; Buchholz, A.; Plass, W. *Eur. J. Inorg. Chem.* **2005**, 4875. (l) Liu, Y.; Xuan, W.; Zhang, H.; Cui, Y. *Inorg. Chem.* **2009**, *48*, 10018.

Published on Web 10/01/2010

Chart 1

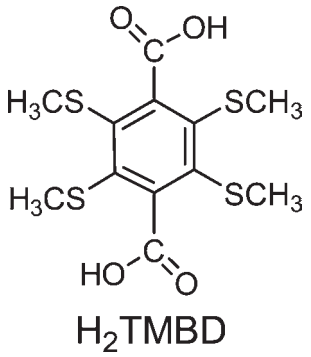

H_2TMBD

coordination networks,[3] and more recently initiated a preliminary study on the advantages of combining the chemically hard carboxyl and chemically soft thioether/thiol functions in the design of organic building blocks for coordination networks.[4] For example, the chemically hard, ionic carboxylate groups are often predisposed as the primary group to interact with metal ions (preferably ones with sufficient chemical hardness) for network formation, while leaving the neutral, and generally weaker-binding thioether groups as free-standing, secondary donors. In previous communications,[4a,b,d] we have demonstrated the viability of building open metal-carboxylate networks containing free-standing methylthio groups (i.e., $Zn_4O(H_2O)_3(TMBD)_3$ and PbTMBD, with TMBD being the tetrakis(methylthio)-benzenedicarboxylate ligand, see Chart 1) that led to effective binding for a metal guest such as $HgCl_2$.

To further explore the rich potential offered by the interplay of the thioether-carboxyl duo, we here report two new network compounds from TMBD and copper ions. Compound **1** presents a rare case in which the metal ion (i.e., Cu^+) is exclusively bonded to the sulfur atoms, while the carboxyl units remain, quite notably, uncoordinated. Compound **2**, on the other hand, is a mixed-cation network containing both Cu^+ and Cu^{2+} ions, with the former being coordinated to the sulfur functions, and the latter to the carboxylate units. Juxtaposed with the previously reported compound Cu_2TMBD,[4a] in which the Cu(I) ion is simultaneously bonded to the carboxylate and thioether groups, these structures present a well-defined evolution in the bonding patterns of the thioether-carboxyl duo. In a preliminary property study, we discovered that the crystals of compound **2**, in spite of the apparent lack of open channels, exhibit an effective absorption of ammonia gas, concomitant with a distinct color change of the crystals. The structural integrity of the network remains intact in the absorption process, thus providing a new case of dynamic transport of molecules in non-porous crystals, a phenomenon that is of current interest across the fields of molecular and solid state materials.[1e,j,5]

Table 1. X-ray Crystallographic Data for **1** and **2**

	1	**2**
formula	$C_{24}H_{27}CuO_8S_8$	$C_{24}H_{29}Cu_3O_{11}S_8$
temperature (K)	100(2)	100(2)
fw	763.57	940.57
space group	$P\bar{1}$	$P2_1/n$
a, Å	9.6326(7)	13.170(2)
b, Å	13.433(1)	19.930(2)
c, Å	13.478(1)	13.175(2)
α, deg	91.952(1)	90
β, deg	110.519(1)	105.523(2)
γ, deg	109.606(1)	90
V, Å^3	1515.6(2)	3332.0(7)
Z	2	4
ρ_{calcd}, (g/cm^3)	1.673	1.875
wavelength, Å	0.71073 (Mo Kα)	0.71073 (Mo Kα)
abs coeff (μ, mm^{-1})	1.318	2.455
$R_1{}^a$ [$I > 2\sigma(I)$]	2.82%	4.20%
$wR_2{}^b$ [$I > 2\sigma(I)$]	6.47%	9.79%

$^a R_1 = \sum||F_o| - |F_c||/\sum|F_o|$. $^b wR_2 = \{\sum w(F_o^2 - F_c^2)^2/\sum w(F_o^2)^2\}^{1/2}$.

Experimental Details

Starting materials, reagents, and solvents were purchased from commercial sources (Aldrich and Acros) and used without further purification. Elemental analysis was performed by a Vario EL III CHN elemental analyzer. FT-IR spectra were measured using a Nicolet Avatar 360 FT-IR spectrophotometer. Thermogravimetric analysis (TGA) was carried out in a nitrogen stream using PerkinElmer STA6000 thermal analysis equipment with a heating rate of 10 °C min^{-1}. Powder X-ray diffraction (XRD) patterns of the bulk samples (the powder samples were spread onto glass slides for data collection) were collected at room temperature on a Siemens D500 powder diffractometer for compound **1** (Supporting Information, Figure S1), and a Bruker D8 Advance diffractometer for compound **2** (both with Cu Kα, λ = 1.5418 Å). The program Mercury was used in the calculation of powder patterns from single crystal structures.

Magnetic susceptibility measurements were obtained with the use of a Quantum Design SQUID magnetometer MPMS-XL. This magnetometer works between 1.8 and 400 K for direct current (dc) applied fields ranging from −7 to 7 T. Measurements were performed on a microcrystalline sample of 19.99 mg for **2**. Prior to the complete study, an M versus H measurement was performed at 100 K to confirm the absence of ferromagnetic impurities. The magnetic data were corrected for the sample holder and the diamagnetic contributions.

Single crystal XRD analyses (data collection, structure solution, and refinement) were conducted on a Bruker AXS SMART APEX CCD system using Mo Kα (λ = 0.71073 Å) radiation at 100(2) K (Table 1). All absorption corrections

(3) (a) Xu, Z. *Coord. Chem. Rev*. **2006**, *250*, 2745. (b) Li, K.; Xu, Z.; Xu, H.; Carroll, P. J.; Fettinger, J. C. *Inorg. Chem*. **2006**, *45*, 1032. (c) Sun, Y.-Q.; He, J.; Xu, Z.; Huang, G.; Zhou, X.-P.; Zeller, M.; Hunter, A. D. *Chem. Commun*. **2007**, 4779. (d) Huang, G.; Xu, H.; Zhou, X.-P.; Xu, Z.; Li, K.; Zeller, M.; Hunter, A. D. *Cryst. Growth Des*. **2007**, *7*, 2542. (e) Sun, Y.-Q.; Tsang, C.-K.; Xu, Z.; Huang, G.; He, J.; Zhou, X.-P.; Zeller, M.; Hunter, A. D. *Cryst. Growth Des*. **2008**, *8*, 1468. (f) Huang, G.; Yang, C.; Xu, Z.; Wu, H.; Li, J.; Zeller, M.; Hunter, A. D.; Chui, S. S.-Y.; Che, C.-M. *Chem. Mater*. **2009**, *21*, 541. (g) Huang, G.; Tsang, C.-K.; Xu, Z.; Li, K.; Zeller, M.; Hunter, A. D.; Chui, S. S. Y.; Che, C.-M. *Cryst. Growth Des*. **2009**, *9*, 1444.

(4) (a) Zhou, X.-P.; Xu, Z.; Zeller, M.; Hunter, A. D.; Chui, S. S.-Y.; Che, C.-M. *Inorg. Chem*. **2008**, *47*, 7459. (b) Zhou, X.-P.; Xu, Z.; Zeller, M.; Hunter, A. D. *Chem. Commun*. **2009**, 5439. (c) He, J.; Yang, C.; Xu, Z.; Zeller, M.; Hunter, A. D.; Lin, J. *J. Solid State Chem*. **2009**, *182*, 1821. (d) Zhou, X.-P.; Xu, Z.; Zeller, M.; Hunter, A. D.; Chui, S. S.-Y.; Che, C.-M.; Lin, J. *Inorg. Chem*. **2010**, *49*, 7629.

(5) (a) Southon, P. D.; Liu, L.; Fellows, E. A.; Price, D. J.; Halder, G. J.; Chapman, K. W.; Moubaraki, B.; Murray, K. S.; Létard, J.-F.; Kepert, C. J. *J. Am. Chem. Soc*. **2009**, *131*, 10998. (b) Kepert, C. J.; Prior, T. J.; Rosseinsky, M. J. *J. Am. Chem. Soc*. **2000**, *122*, 5158. (c) Kepert, C. J. *Chem. Commun*. **2006**, 695. (d) Bradshaw, D.; Prior, T. J.; Cussen, E. J.; Claridge, J. B.; Rosseinsky, M. J. *J. Am. Chem. Soc*. **2004**, *126*, 6106. (e) Zhao, X.; Xiao, B.; Fletcher, A. J.; Thomas, K. M.; Bradshaw, D.; Rosseinsky, M. J. *Science* **2004**, *306*, 1012. (f) Biradha, K.; Hongo, Y.; Fujita, M. *Angew. Chem., Int. Ed*. **2002**, *41*, 3395. (g) Zhang, J.-P.; Chen, X.-M. *J. Am. Chem. Soc*. **2008**, *130*, 6010. (h) Kawano, M.; Fujita, M. *Coord. Chem. Rev*. **2007**, *251*, 2592. (i) Atwood, J. L.; Barbour, L. J.; Jerga, A.; Schottel, B. L. *Science* **2002**, *298*, 1000. (j) Tian, J.; Thallapally, P. K.; Dalgarno, S. J.; Atwood, J. L. *J. Am. Chem. Soc*. **2009**, *131*, 13216. (k) Dobrzanska, L.; Lloyd, G. O.; Raubenheimer, H. G.; Barbour, L. J. *J. Am. Chem. Soc*. **2006**, *128*, 698. (l) Barbour, L. J. *Chem. Commun*. **2006**, 1163.

were performed using the SADABS program. The structures were solved and refined by full-matrix least-squares on F_o^2 using SHELXL 6.14 (Bruker AXS Inc., Madison, Wisconsin, U.S.A., 2003). The structure of **2** emulates a double volume C-centered orthorhombic cell with the values $a = 15.942$, $b = 20.974$, and $c = 19.930$ Å and is pseudomerohedrally twinned. Application of the matrix 0 0 −1, 0 −1 0, −1 0 0 results in a twin ratio of 0.6842(8) to 0.3058(8). Three of the methylthio groups are disordered over two moieties with each mutually exclusive positions with an occupancy rate for the major moiety of 0.531(4). Equivalent disordered C−S bonds were restrained to be the same within a standard deviation of 0.02 Å, and the atoms C21, C24, and S5 were constrained to have the same ADPs as their disordered counterparts.

Synthesis of the H_2TMBD Ligand. This was based on a reported method.[4a]

Crystallization of 1. A mixture of $Cu(NO_3)_2 \cdot 3H_2O$ (24.0 mg, 0.10 mmol), H_2TMBD (35.0 mg, 0.10 mmol), and water (5.0 mL) were sealed in a 20 mL Teflon-lined reactor in an oven at 140 °C for 48 h and slowly cooled to room temperature within 12 h. Light-yellow block crystals of diffraction quality were obtained (14.3 mg, 38% based on H_2TMBD). Significant redox reaction between the Cu(II) species used and the TMBD molecules apparently occurred to generate, in situ, the Cu(I) species for the formation of compound **1**. Powder XRD of the product indicated a single phase consistent with the single crystal structure (Supporting Information, Figure S1). Chemical analysis of the product $C_{24}H_{27}CuO_8S_8$ [corresponding to $Cu(TMBD)_{0.5}$-$(H_2TMBD)_{0.5} \cdot H_2TMBD$] yields the following: found [C (37.69%), H (3.54%)]; calcd [C (37.75%), H (3.56%)]. IR ($\bar{\nu}$/cm^{-1}): 3430w, 2994w, 2920w, 2530w, 2438w, 1744s, 1721s, 1636s, 1415s, 1377s, 1301s, 1224s, 1125w, 1106w, 971s, 915s, 782s, 694m, 618w, 581w, 428w.

Crystallization of Cu_2TMBD. A mixture of $Cu(NO_3)_2 \cdot 3H_2O$ (3.0 mg, 0.012 mmol), H_2TMBD (3.5 mg, 0.010 mmol), and water (0.5 mL) were sealed in a glass tube and heated in an oven at 140 °C for 48 h and slowly cooled to room temperature at a rate of 5 °C h^{-1}. Yellow needle-like crystals of diffraction quality were obtained (26% based on H_2TMBD). Significant redox reaction between the Cu(II) species used and the TMBD molecules apparently occurred to generate the Cu(I) species for the formation of Cu_2TMBD. Experiments on larger scales (e.g., with 20.0 mg of TMBD) in a 20-mL Teflon-lined reactor provided the same product in single phase purity (as checked by powder XRD). Chemical analysis of the product $C_6H_6CuO_2S_2$ [corresponding to $Cu(TMBD)_{0.5}$] yields the following: found [C (30.27%), H (2.70%)]; calcd [C (30.31%), H (2.54)]. IR ($\bar{\nu}$/cm^{-1}): 2963w, 2923w, 1578s, 1414s, 1312s, 1261s, 1219w, 1029m, 990w, 970w, 840w, 801m, 779w, 606w.

Crystallization of 2. A mixture of $Cu(NO_3)_2 \cdot 3H_2O$ (15.0 mg, 0.062 mmol), H_2TMBD (9.0 mg, 0.026 mmol), and water (2.0 mL) were sealed in a Pyrex glass tube in an oven at 140 °C for 48 h and slowly cooled to room temperature within 12 h. Green block crystals of diffraction quality were obtained (4.5 mg, 37% based on H_2TMBD). Significant redox reaction between the Cu(II) species used and the TMBD molecules apparently occurred to generate the Cu(I) species for the formation of compound **2**. X-ray powder diffraction of the product indicated a single phase consistent with the single crystal structure (vide infra). Chemical analysis of the product $C_{24}H_{29}Cu_3O_{11}S_8$ [corresponding to $Cu^{II}_2OHCu^{I}(TMBD)_2 \cdot 2H_2O$] yields the following: found [C (30.71%), H (3.12%)]; calcd [C (30.68%), H (3.00%)]. IR ($\bar{\nu}$/cm^{-1}): 3411w, 2987w, 2923w, 1600s, 1438s, 1310s, 1123w, 1053w, 973 m, 784w, 624w.

Ammonia Treatment of 2. The ammonia gas used here was generated from anhydrous liquid ammonia in a stainless-steel cylinder (Arkonic Gases & Chemicals Inc.). A septum-capped round bottomed flask (100 mL) containing the crystals of **2** (5.0 mg, placed in an uncapped vial for easy collection) was purged by the ammonia gas (e.g., by passing NH_3 in from one needle and out through another for about 5 min). The crystal sample was kept under this atmosphere of ammonia for 1 h, and the individual crystallites became uniformly blue in appearance. Elemental analysis of the ammonia-treated sample of **2** found [C (29.64%), H (3.40%), N (1.76%)]. The elemental profile is consistent with the formula $Cu^{II}_2OHCu^{I}(TMBD)_2 \cdot NH_3 \cdot 3H_2O$: calcd [C (29.54%); H (3.51%), N (1.44%)]. Because of the relatively small nitrogen content, the number of NH_3 (and to some degree H_2O) molecules thus derived in the formula is only semiquantitative. Additional support for the formula was obtained from the TGA plot for the ammonia-treated sample of **2** (Supporting Information, Figure S2), in which the first-stage weight loss of 5.4% at about 76 °C is consistent with the weight percentage of the three guest water molecules for $Cu^{II}_2OHCu^{I}(TMBD)_2 \cdot NH_3 \cdot 3H_2O$ (calculated: 5.5%).

Methylamine Treatment of 2. A small vial containing about 5.0 mg of solid **2** was placed into a larger vial containing about 1.0 mL of methylamine (33% wt. solution in absolute ethanol), with care being taken to avoid direct contact between the solid sample and the liquid. The larger vial was then capped to facilitate the vapor treatment experiment. The duration of the vapor treatment was 1.0 h. Elemental analysis of the methylamine-treated sample of **2** found [C (29.99%), H (4.71%), N (5.17%)], corresponding to $Cu^{II}_2OHCu^{I}(TMBD)_2 \cdot 4MeNH_2 \cdot 5H_2O$: calcd [C (30.08%), H (4.95%), N (5.01%)].

Ethylamine Treatment of 2. A small vial containing about 5.0 mg of solid **2** was placed into a larger vial containing about 1.0 mL of ethylamine (70% wt. solution in water), with care being taken to avoid direct contact between the solid sample and the liquid. The larger vial was then capped to facilitate the vapor treatment experiment. The duration of the vapor treatment was 1.0 h. Elemental analysis of ethylamine-treated sample of **2** found [C (30.55%), H (5.05%), N (4.18%)], corresponding to $Cu^{II}_2OHCu^{I}(TMBD)_2 \cdot 3.2CH_3CH_2NH_2 \cdot 7.5H_2O$]: calcd [C (30.84%), H (5.31%), N (3.79%)].

Results and Discussion

Structure and Characterization of 1. The hydrothermal reaction of $Cu(NO_3)_2 \cdot 3H_2O$ and H_2TMBD in a 1:1 molar ratio in water at 140 °C for 2 days afforded light-yellow, air-stable crystals of **1**. X-ray single-crystal analysis reveals a formula of $Cu_2(TMBD)(H_2TMBD) \cdot 2H_2TMBD$, in which the Cu(I) ions apparently resulted from a redox reaction between the Cu(II) species and the organic sulfide units of the TMBD molecule, a reaction that often occurs under the conditions of hydro(solvo)thermal reactions.[4c,6] The crystal structure of **1** consists of two distinct domains: (1) a 1D chain-like structure based on chelations between the Cu(I) ion and thioether groups of the TMBD and H_2TMBD molecules; (2) individual H_2TMBD molecules that are not bonded to the Cu(I) ions. A total of four crystallographically inequivalent TMBD moieties are found, two on the chain and two among the non-coordinated TMBD molecules (see Figure 1). The Cu(I) atom, adopting a distorted tetrahedral geometry, is bound by two TMBD molecules via the *para*-bis(methylthio) units, with Cu−S distances ranging from 2.253 to 2.335 Å. Among the two coordinated molecules, one appears to be in the acid (fully protonated) form, while the other is dianionic and thus serves to balance the charge of the Cu^+ centers. Such consideration is supported by the C−O distances in the carboxyl groups. Specifically, in the acid form, the two C−O distances observed are quite different (i.e., C16−O6, 1.206 Å; C16−O5, 1.317 Å, suggesting O5 is

(6) Chen, X.-M.; Tong, M.-L. *Acc. Chem. Res.* **2007**, *40*, 162.

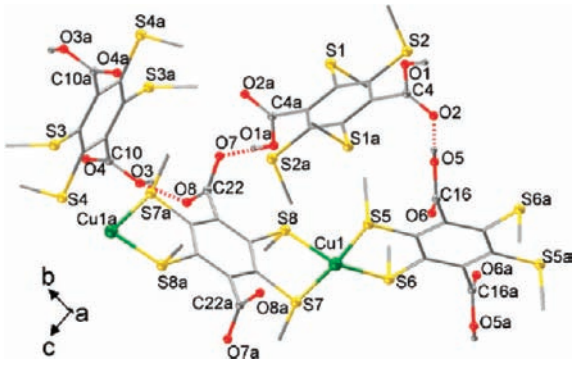

Figure 1. Four TMBD molecules and two associated Cu(I) ions in **1** with atom labeling (crystallographically equivalent atoms are differentiated by the letter a). The H-bonds are shown as dotted red lines. H atoms of the methyl groups are omitted for clarity.

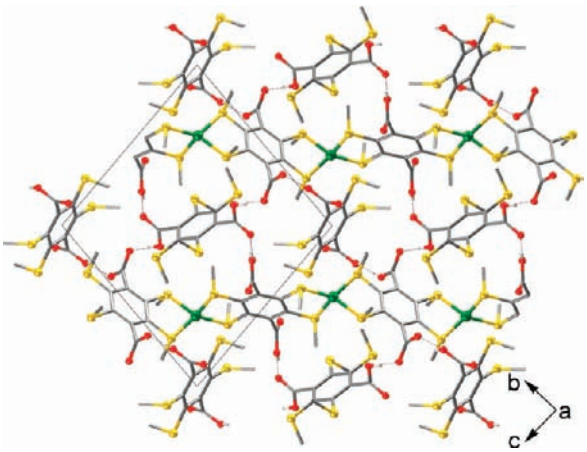

Figure 2. Overview of the structure of **1** along the *a* axis. Green spheres, Cu(I); yellow, S; red, O.

protonated), whereas the dianionic form features more similar C−O distances (i.e., C22−O7, 1.231 Å; C22−O8, 1.272 Å). The O atoms in the anionic form are hydrogen bonded to the non-coordinated TMBD molecules at short O−O distances (i.e., O7−O1, 2.436; O8−O3, 2.609 Å). The acid form on the chain is also hydrogen bonded to one of the non-coordinated TMBD molecules (i.e., O2−O5, 2.560 Å). The strong H-bonds to the anionic carboxylate groups apparently reduce its tendency to bond to the Cu(I) center, and help to create the current structure in which H-bonds and Cu(I)-S coordination bonds jointly integrate the molecular components into 3D composite networks (Figure 2).

The presence of both the acid and anionic forms of the TMBD molecules in **1** is also consistent with the IR spectrum of the solid sample. As seen in Supporting Information, Figure S3, besides the typical, broad O−H stretch of carboxylic acid in the region 3300−2548 cm^{-1}, three intense peaks associated with carbonyl stretches (C═O) can be identified, two at the higher wave numbers of 1744 cm^{-1} and 1721 cm^{-1}, and one at 1650 cm^{-1} (by comparison, H_2TMBD features only one peak for C═O stretching at 1690 cm^{-1}). The higher ones can be ascribed to the C═O stretching bands of the acid forms, and the lower one to the anionic form, as is consistent with the general observation that anionic carboxylate groups feature lower frequency C═O stretching vibrations than the free acid form.[7]

Structure and Characterization of Cu_2TMBD. The previously reported air-stable compound Cu_2TMBD was made with $Cu(NO_3)_2\cdot 3H_2O$ and H_2TMBD in the molar ratio 1.25:1 under similar conditions, and features a 3D coordination network in which the Cu(I) ion is simultaneously bonded to the thioether and carboxylate groups (see Figure 3). The identity and purity of the compound was verified by powder and single crystal XRD as well as IR spectroscopy. The reader is referred to a previous communication for more structural details on this compound.[4a]

Structure and Characterization of 2. The reaction of $Cu(NO_3)_2\cdot 3H_2O$ and H_2TMBD in a molar ratio 2.4:1, namely, by further increasing the relative amount of the Cu(II) salt, afforded green, air-stable crystals of compound **2**. X-ray single-crystal analysis suggests a composition of $Cu^{II}_2OCu^{I}(TMBD)_2\cdot H^+\cdot 2H_2O$. Notice that the H^+ species cannot be located from the current X-ray data set; its presence is deduced from a charge balance requirement, and the H^+ species could be associated with the water molecules or the complex. In this reaction, the use of larger amounts of Cu(II) species apparently facilitated its incorporation into the solid state product to form the mixed-cation network of **2**.

The formula $Cu^{II}_2OCu^{I}(TMBD)_2\cdot H^+\cdot 2H_2O$ [or $Cu^{II}_2OHCu^{I}(TMBD)_2\cdot 2H_2O$] is supported by the results of elemental analyses, and the Cu^{II} and Cu^{I} mixed-cation feature is verified by magnetic measurements (see below). TGA measurement (Supporting Information, Figure S2) on an as-made sample of **2** reveals an accumulated weight loss of about 1.94% at up to 200 °C, which corresponds to the weight percentage of one water molecule (1.91%) for $Cu^{II}_2OHCu^{I}(TMBD)_2\cdot 2H_2O$. The TGA results thus indicate that half of the water molecules in **2** are resistant against evacuation by heat. This is consistent with the presence of two crystallographically inequivalent water molecules in the crystal structure: one (that of O11) is situated 3.610 Å from a Cu^{II} center (Cu1), indicating a certain degree of coordination; the other (that of O10), by comparison, is not associated with the Cu ions at all. We ascribe the low volatility to the O11 water molecule, and for this we conjure up the following scenario: upon heating, the crystal lattice flexes and allows for this H_2O to access more closely the Cu^{II} center, which, at higher temperatures, eventually leads to the highly stable cupric hydroxide species [e.g., $Cu(OH)^+$, together with some form of the carboxylic acid group (−COOH) on TMBD].

The Cu(II) ions in the crystal structure of **2** are aggregated into a centrosymmetric tetranuclear core $Cu^{II}_4O_2$ (Figure 4a). The $Cu^{II}_4O_2$ core features two μ_3-bridged O atoms, which bond to two Cu^{II} ions (labeled Cu1) to form a 4-member ring (Cu−O distances: 1.967 and 1.978 Å). The other two Cu^{II} ions (labeled Cu2) are bonded to the μ_3-O atoms at distances of 1.962 Å. The $Cu^{II}_4O_2$ units are bound by eight carboxylate groups (each from an individual TMBD molecule) to furnish the square-pyramidal coordination spheres of the Cu^{II} atoms. Only a thioether sulfur atom at 3.970 Å and an aqua O atom at 3.610 Å were found off the base of the square pyramid, suggesting certain accessibility of the Cu^{II} centers from this direction, which,

(7) Günzler, H.; Gremlich, H.-U. *IR Spectroscopy: An Introduction*; Wiley: Weinheim, 2002.

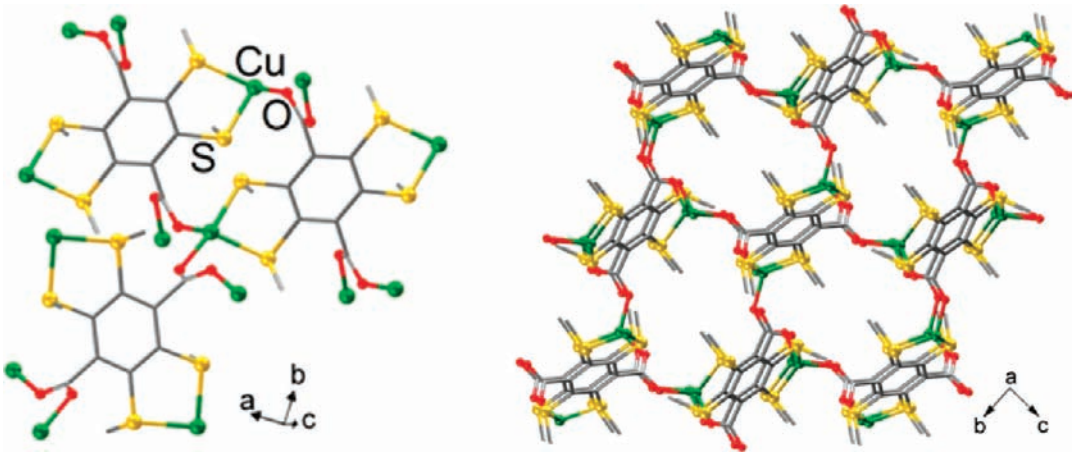

Figure 3. Local coordination environment of ligand TMBD and Cu(I) centers (left), and an overview of the 3D coordination network of Cu_2TMBD (right).

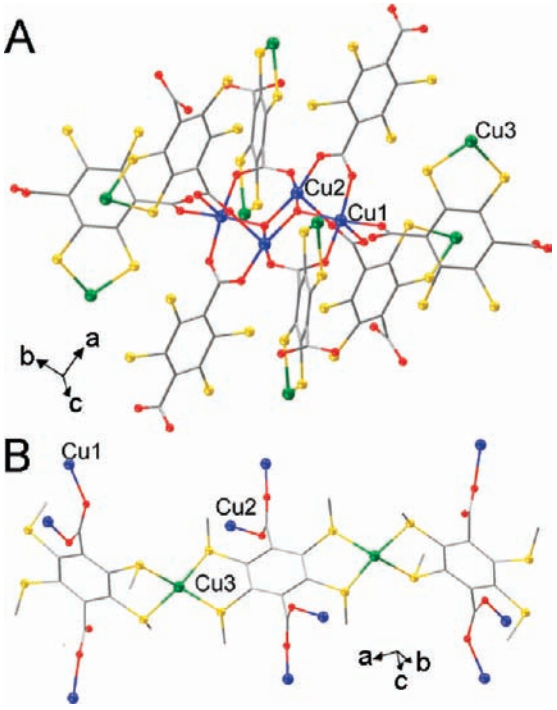

Figure 4. Local bonding environment in **2**. (a) The $Cu^{II}_4O_2$ core and the associated TMBD ligands (8 of them) and Cu(I) centers. (b) The Cu^{I}_2-$(TMBD)_3$ unit of two Cu^{I} ions and three TMBD molecules.

as will be seen later, might in part account for the sensitive color change of this crystal upon exposure to ammonia.

The cuprous (Cu^{I}) center is bound by a pair of methylthio groups from the TMBD molecules (Cu−S distances: from 2.282 to 2.323 Å), featuring a distorted tetrahedral geometry like in compound **1** (Figure 4b), with a carbonyl O atom remotely situated 3.624 Å away. Among the eight TMBD molecules coming off each $Cu^{II}_4O_2$ complex, two are each bonded to two Cu^{I} centers (using both pairs of methylthio groups), four are each bonded to one Cu^{I} center, and the remaining two are not bonded to Cu^{I} (leaving all its four S atoms free-standing, Figure 4a). The multiple metal-carboxylate connections coming off the $Cu^{II}_4O_2$ unit, together with the Cu^{I}−S links, present an overwhelmingly complex network at first glance (Figure 5).

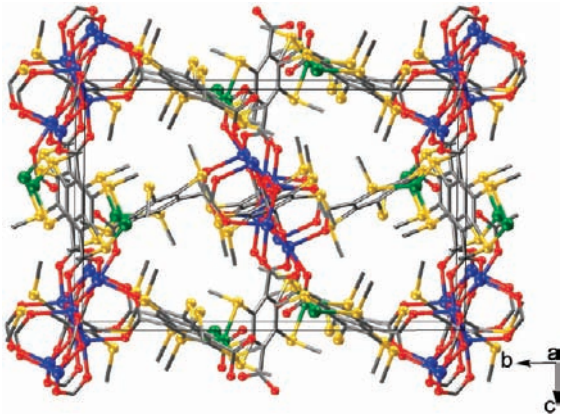

Figure 5. View of the crystal structure of **2** along the *a* axis. Blue spheres, Cu^{II}; green, Cu^{I}; yellow, S; red, O.

An analysis of the connectivity of this intricate network can be undertaken in two steps. First, one omits the Cu(I) centers, and treats the $Cu^{II}_4O_2$ units as 8-connected nodes connected by the TMBD molecules as linear rods. This gives an 8-connected net similar to a reported 8-connected Ln network,[8] which can be further decomposed into two sets of intersecting (4, 4) nets; the nets within each individual set are parallel to one another (as shown in Figure 6a, one set runs nearly horizontal, and the other vertical). In the second step, one turns to the Cu(I) centers and the associated TMBD molecules (see Figure 4b); these distinctly constitute a trimeric unit: one TMBD flanked by two Cu(I) ions, which are each in turn capped by a TMBD molecule (the capping TMBD is bonded to only one Cu^{I}). This $Cu^{I}_2(TMBD)_3$ unit can then be considered a 6-connected node—a building block with six carboxylate groups, each bonded to a different $Cu^{II}_4O_2$ core. On the basis of the connections between the $Cu^{I}_2(TMBD)_3$ unit and the $Cu^{II}_4O_2$ unit thus established, one obtains a 3D net with two types of 6-connected nodes that is comparable to the relatively rare roa topology (Figure 6b).[9]

(8) Hill, R. J.; Long, D.-L.; Champness, N. R.; Hubberstey, P.; Schröder, M. *Acc. Chem. Res.* **2005**, *38*, 335.

(9) Zhong, R.-Q.; Zou, R.-Q.; Du, M.; Jiang, L.; Yamada, T.; Maruta, G.; Takeda, S.; Xu, Q. *CrystEngComm* **2008**, *10*, 605.

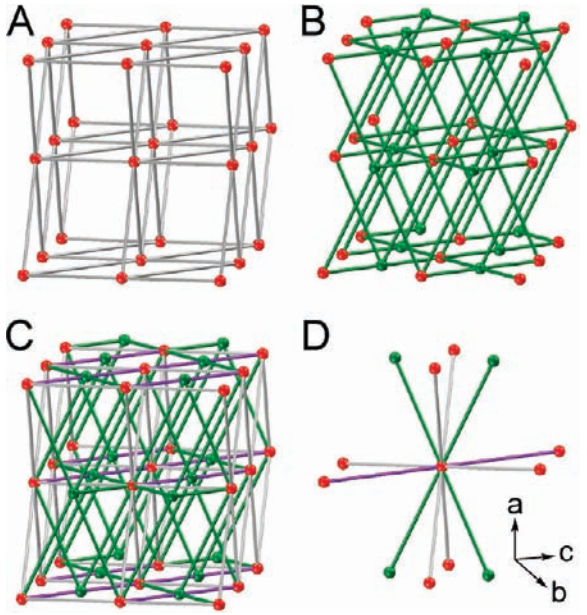

Figure 6. Topological representation of the network in **2**. (a) The 8-connected net based on the $Cu^{II}_4O_2$ cluster as the node and the TMBD molecules as the struts. (b) The 6-connected net derived from linking the $Cu^{I}_2(TMBD)_3$ unit (Figure 4b) as a 6-connected node with the $Cu^{II}_4O_2$ cluster (as a 6-connected node here). (c) An overall view showing both the 8-connected net and the 6-connected net (the purple rods denote the connections shared by both nets). (d) A local view of the $Cu^{II}_4O_2$ center as a 12-connected node. Red and green spheres denote the geometric centers of the $Cu^{II}_4O_2$ and $Cu^{I}_2(TMBD)_3$ units, respectively.

The 8-connected net and the roa net intersect at the $Cu^{II}_4O_2$ nodes to provide the seemingly intricate overall connectivity (Figure 6c), with each $Cu^{II}_4O_2$ node having a total of 12 connections: 6 from the 8-connected net (shown in gray in Figure 6d), 4 from the roa net (green), and the remaining two (purple) are shared by the two constituent nets. In other words, the 8-connected net and the roa net not only intersect at the $Cu^{II}_4O_2$ nodes, but also overlap in two of the struts (around each node).

No open channels are observed in the structure of **2**, and the solvent accessible region accounts for only 4.0% of the cell volume (calculated from PLATON,[10] with the two water guests excluded). The solvent accessible region contains the water molecules in the pristine samples. As will be seen below, it is this small fraction of solvent accessible region that might, in a large measure, account for the absorption behavior of this compound in relation to ammonia.

Magnetic Properties of 2. Magnetic susceptibility measurements were conducted to further verify the presence of both Cu(II) and Cu(I) ions in compound **2**, and to examine the magnetic interactions thereof.

At room temperature, the χT product value is 1.76 cm^3 K/mol (Figure 7). This value is in good agreement with the expected Curie constant for four Cu(II) $S = 1/2$ spins (1.5 cm^3 K/mol) and a g value above 2 as expected for Cu(II) systems. When the temperature is lowered, the χT product continuously decreases down to 1.8 K reaching 0.16 cm^3 K/mol suggesting a singlet ground state for the tetranuclear Cu(II) units. On the basis of the structure,

(10) Spek, A. L. *PLATON, A Multipurpose Crystallographic Tool*; Utrecht University: Utrecht, The Netherlands, 2001.

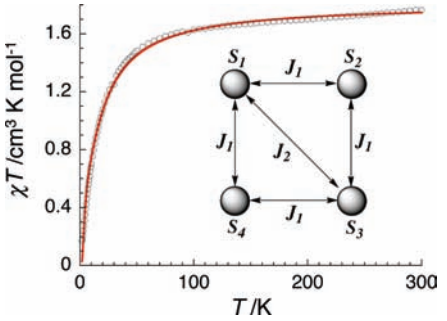

Figure 7. Temperature dependence of the χT product (χ being the magnetic susceptibility defined as M/H per complex) for **2** under the applied fields of 1000 Oe. The solid red line is the best fit obtained with a tetranuclear Heisenberg model of isotropic $S = 1/2$ spins (see text). Inset: A schematic of the magnetic coupling topology in the tetranuclear Cu(II) complex in **2**.

the complexes can be magnetically viewed as tetramers of $S = 1/2$ Cu(II).

The application of the van Vleck equation[11] to the Kambe's vector coupling scheme[12] allows the determination of an analytical expression of the magnetic susceptibility from the following spin Hamiltonian:

$$H = -2J_1\{S_1\cdot S_2 + S_2\cdot S_3 + S_3\cdot S_4 + S_1\cdot S_4\} - 2J_2\{S_1\cdot S_3\} \quad (1)$$

where S_i are the spin operators ($S = 1/2$ for Cu), J_1 and J_2 are defined by the scheme in the inset of Figure 7. The expression of the susceptibility can be deduced from the literature.[13] Then the analytical expression of the magnetic susceptibility is:

$$\chi_{Cu_4} = \frac{2Ng^2\mu_B^2}{k_BT}\frac{e^{2J_1/k_BT} + e^{4J_1-2J_2/k_BT} + e^{4J_1/k_BT} + 5e^{6J_1/k_BT}}{1 + 3e^{2J_1/k_BT} + 4e^{4J_1-2J_2/k_BT} + 3e^{4J_1/k_BT} + 5e^{6J_1/k_BT}} \quad (2)$$

As shown in Figure 7, the above model reproduces very well the experimental data with $J_1/k_B = -16(1)$ K, $J_2/k_B = -22(3)$ K and $g = 2.19(2)$ (red line). The sign of the magnetic interactions confirms the $S_T = 0$ ground state of the $Cu^{II}_4O_2$ units.

Response of Compound 2 to NH_3 gas. In spite of the lack of open channels in its crystal structure, crystal samples of **2** exhibit a distinct response to ammonia. Upon exposure to ammonia gas for 1 h, the green crystals of **2** (as-made samples, no grinding applied) become blue in color (Figure 8). The color change from green to blue appears to be consistent with a stronger ligand field around the Cu(II) centers. The strengthening of the ligand field could arise from the ammonia reacting with the H^+ species in the structure (thus enhancing the bonding of the oxo ligands), or the ammonia binding directly to the Cu(II) centers. Notice that, in general, amine complexes of Cu(II) are generally more intensely blue than the aqua ion;

(11) van Vleck, J. H. *The Theory of Electric and Magnetic Susceptibility*; Oxford University Press: London, 1932.
(12) Kambe, K. *J. Phys. Soc. Jpn.* **1950**, *5*, 48.
(13) Hall, J. W.; Estes, W. E.; Estes, E. D.; Scaringe, R. P.; Hatfield, W. E. *Inorg. Chem.* **1977**, *16*, 1572.

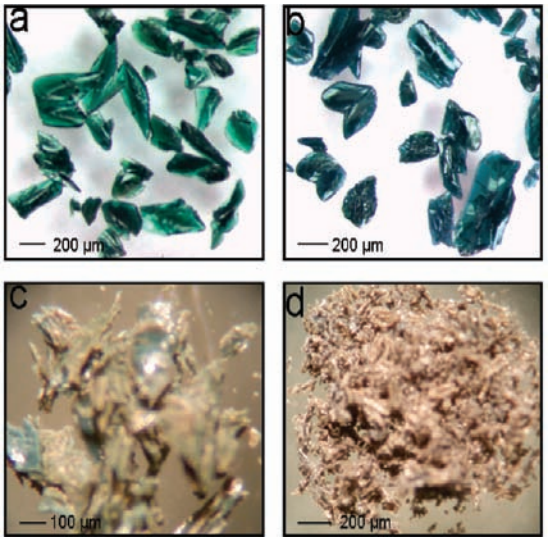

Figure 8. Photographs of as-made crystals of **2** (a), and crystals of **2** after being immersed in an ammonia atmosphere for 1 h (b), in a methylamine atmosphere for 1 h (c), and ethylamine atmosphere for 1 h (d).

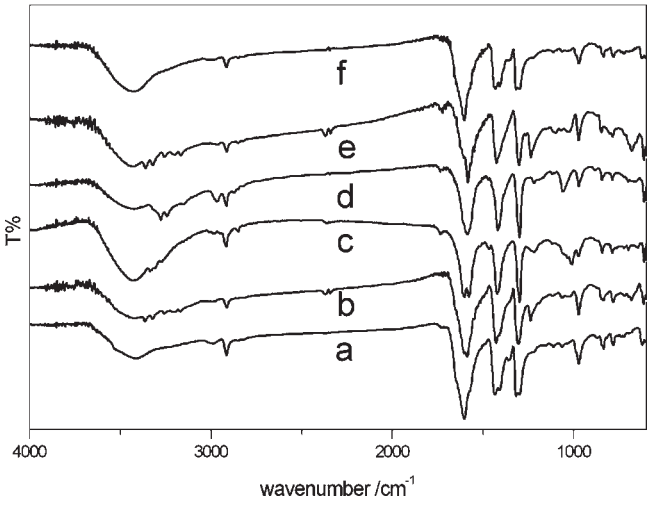

Figure 9. IR spectra of an as-synthesized sample of **2** (a); the sample of (a) immersed for 1 h in an NH_3 atmosphere (b), in methylamine (c), and ethylamine vapor (d); the sample of (b) after heating at 130 °C in a vacuum for 4.0 h (e); and a sample of (a) immersed in an H_2S atmosphere for 1 h (f).

the amines produce a stronger ligand field, causing the absorption band to move from the far red to the middle of the red region of the spectrum.[14] Our current data, however, can not pinpoint the NH_3 molecules in the structure, and the rigorous determination of the mechanism that underlies the color change would involve a more elaborate study (e.g., a single crystal structure that locates the NH_3 molecules and reveals the bonding environment around the Cu^{II} centers).

Additional evidence in support of the uptake of NH_3 is provided by elemental analyses (Experimental Section) and IR measurements. As seen in Figure 9, peaks of N−H stretching are observed in the region of 3150 cm^{-1} to 3365 cm^{-1}, for the ammonia-treated sample (spectrum b in Figure 9), whereas in the pristine sample, such peaks are

(14) Cotton, F. A.; Wilkinson, G.; Murillo, C. A.; Bochmann, M. *Advanced Inorganic Chemistry*, 6th ed.; John Wiley & Sons, Inc.: New York, 1999; p 868.

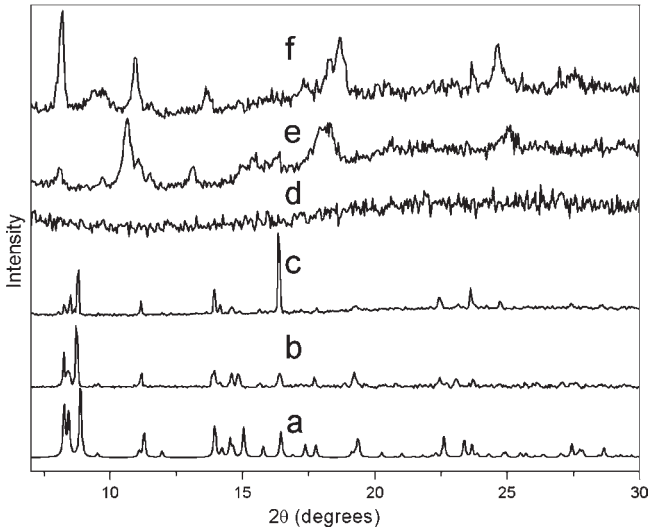

Figure 10. XRD patterns (Cu Kα, $\lambda = 1.5418$ Å): calculated from the single-crystal structure of **2** with random orientation of crystallites (a); observed for an as-synthesized powder solid of **2** (b); observed for a sample of (b) immersed in an NH_3 atmosphere for 1.0 h (c); sample of (c) after heating at 160 °C in a vacuum for 4.0 h (d); observed for a sample of (b) immersed in methylamine vapor (e), and in ethylamine vapor for 1.0 h (f).

absent (spectrum a in Figure 9). Moreover, the crystals of **2** remained transparent with the same morphology (very little cracking) after the ammonia treatment, and powder XRD indicates that the original lattice was retained (pattern c, Figure 10). The transport of ammonia molecules throughout the seemingly channel-free structure of **2** reflects the structural dynamics and flexibility of the host network, a type of solid state property that has received increasing attention.[1e,j,5] In these dynamic processes, the diffusion of guest species is probably accompanied by significant structural changes in the host networks, which often serves to modify and assist the transport of the guest molecules.

Attempts to remove NH_3 from the crystalline host of **2** were not successful. For example, after heating the NH_3-loaded crystals at 130 °C in a vacuum for 4 h, the IR measurement continued to feature the peaks of N−H vibration (spectrum e in Figure 9). Heating at higher temperatures (e.g., 160 °C), however, led to disintegration of the host net, as is revealed by powder X-ray studies (pattern d, Figure 10).

Treatment with the larger-size methylamine and ethylamine, by comparison, proved to be much more disruptive: the crystals of **2** disintegrate into lackluster, brownish powdery products (Figure 8c,d), with the original lattice decidedly destroyed, to make way for unknown, albeit crystalline phases (see powder patterns e and f in Figure 10). Elemental analysis also revealed significantly a higher nitrogen content than in the NH_3-treated compound, indicating a higher molar uptake of the methylamine and ethylamine molecules. Apparently the destruction of the host net removed the spatial constraint for the guest molecules (i.e., the pristine structure of **2** only contains 4% of solvent accessible region), and opens the possibility for a larger number of methylamine or ethylamine molecules to react with compound **2**.

The strong affinity observed of compound **2** for the alkaline molecules of ammonia and amines may be driven

by the existence of acidic H^+ species in the structure of **2**. By comparison, exposure to H_2S gas under similar conditions does not change the color or IR features of crystals of **2** (spectrum f, Figure 9), in spite of the potentially strong reactivity of H_2S toward the Cu(II) and Cu(I) species.

Conclusion

The exploratory studies here help to demonstrate the rich potential of the thioether-carboxyl combination for generating a wide spectrum of novel structural features in coordination networks, as is illustrated in the uncoordinated carboxylic groups in the network of **1**, the simultaneous coordination of the carboxylate and the thioether to Cu^I (as in Cu_2TMBD), the mixed Cu^{II}/Cu^I system of **2**, and the free-standing thioether groups in the open frameworks described elsewhere. In particular, the mixed-cation feature of **2** suggests that the thioether-carboxyl duo might be especially suited for achieving advanced network systems containing mixed metal ion centers (e.g., using a hard ion like Eu^{3+} to bind to the carboxylate and a soft one like Ag^+ or Au^+ for the thioether).[4d] Equipped with the efficient synthetic tools offered by organic chemistry, we foresee many more opportunities for exploiting the interesting potentials of the carboxylate and thioether combination.

Acknowledgment. This work is supported by City University of Hong Kong (Project No. 7002471) and the Research Grants Council of HKSAR [Project 9041322 (CityU 103009)]. The diffractometer was funded by NSF grant 0087210, by the Ohio Board of Regents Grant CAP-491, and by YSU. We also thank the University of Bordeaux, Région Aquitaine, GIS Advanced Materials in Aquitaine (COMET Project), MAGMANet (NMP3-CT-2005-515767) and CNRS for financial supports of the magnetic studies.

Supporting Information Available: Full crystallographic data in CIF format for compounds **1** and **2**, powder XRD patterns for bulk samples of **1**, TGA plots for **2** and ammonia treated sample of **2**, IR spectrum of H_2TMBD, **1** and **2**. This material is available free of charge via the Internet at http://pubs.acs.org.